Accepted Manuscript

Escherichia coli AlkB and single-stranded DNA binding protein SSB interaction explored by Molecular Dynamics Simulation

Monisha Mohan, Vishal Pandya, Roy Anindya

PII: S1093-3263(18)30099-8

DOI: 10.1016/j.jmgm.2018.05.007

Reference: JMG 7172

To appear in: *Journal of Molecular Graphics and Modelling*

Received Date: 12 February 2018

Revised Date: 30 April 2018

Accepted Date: 16 May 2018

Please cite this article as: M. Mohan, V. Pandya, R. Anindya, *Escherichia coli* AlkB and single-stranded DNA binding protein SSB interaction explored by Molecular Dynamics Simulation, *Journal of Molecular Graphics and Modelling* (2018), doi: 10.1016/j.jmgm.2018.05.007.

Escherichia coli AlkB and Single-stranded DNA Binding Protein SSB Interaction Explored by Molecular Dynamics Simulation

Monisha Mohan[a], Vishal Pandya[a], Roy Anindya*[a]

[a] Department of Biotechnology, Indian Institute of Technology Hyderabad, Kandi, Sangareddy, Hyderabad-502285, Telangana, India

* To whom correspondence should be addressed: Roy Anindya, Tel.: +91-40-23016083, Fax: +91-40-23016032, Email: *anindya@iith.ac.in*

Abstract

Repair of alkylation damage in DNA is essential for maintaining genome integrity. *Escherichia Coli* (*E.coli*) DNA repair enzyme AlkB removes methyl adducts including 1-methyladenine and 3-methylcytosine present in DNA by oxidative demethylation from single-stranded DNA (ssDNA). *E.coli* single-stranded DNA binding protein (SSB) selectively binds ssDNA in a sequence-independent manner. We have recently shown that AlkB can repair methyl adduct present in SSB-coated ssDNA. In this study, we aimed to elucidate details of AlkB-mediated DNA repair of SSB-bound DNA substrate. Therefore, we generated a structural model of AlkB-SSB-ssDNA and using Molecular Dynamics simulation analysis we show that flexibility of SSB-bound DNA allows AlkB to bind in multiple ways. Our docking analysis of AlkB-SSB-ssDNA structure revealed that the Cyt109 base is present in the hydrophobic cavity of AlkB active site pocket. The characterization of AlkB-SSB interaction pattern would likely to help in understanding the mode of alkylated DNA adduct recognition by AlkB.

Keywords

Alkylation; AlkB; Fe(II)/2-oxoglutarate-dependent dioxygenase; SSB; DNA repair

Abbreviations

1-methyladenine, 1meA; 3-methlyctosine, 3meC; double-stranded beta-helix (DSBH); High Ambiguity Driven protein Docking, HADDOCK; molecular dynamics, MD; Root mean square fluctuations**,** RMSF; Root mean square deviations**,** RMSD

INTRODUCTION

DNA can be damaged by many endogenous and exogenous agents [1]. Exposure to alkylating agents, especially S_N2 type methylating agents, results in 1-methyladenine (1meA) and 3-methlyctosine (3meC). These adducts are found mainly in ssDNA as these nitrogen atoms are at Watson-Crick base-pairing position in double stranded DNA and generally protected from alkylation damage. The enzyme involved in the repair of these lesions is known as AlkB (Alkylation protein B) in *E.coli*. AlkB is a non-heme iron (Fe^{II}) and 2-oxoglutarate (2OG)-dependent dioxygenases [2]. It catalyzes hydroxylation of alkyl group present on ring nitrogen atoms of DNA bases. These oxidized alkyl groups being inherently unstable released as aldehydes, thus restoring the undamaged adenine and cytosine residues in the DNA [3]. This oxidation reaction is coupled with the decarboxylation of 2OG to form succinate and CO_2. Structural characterizations of AlkB have provided molecular insights into the mechanism of demethylation reaction and substrate recognition [4-6].

Interestingly, AlkB preferentially repairs ssDNA [7]. However, bacterial ssDNA regions are usually stabilized by protein binding, such as, single-stranded DNA-binding protein (SSB). *E. coli* SSB is a tetrameric protein and each monomer has the characteristic DNA binding OB-fold (Oligonucleotide/ oligosaccharide Binding fold) [8] and readily binds ssDNA. For the *E. coli* SSB, two DNA-binding states have been reported [9], one where the tetramer binds to 65 nucleotides at high salt concentration (SSB_{65}), and another where the SSB binds to 35 nucleotides at lower salt concentrations (SSB_{35}). *In vitro* studies established that at NaCl concentration below 20mM predominant binding mode is $(SSB)_{35}$; whereas, at salt concentration of 200mM NaCl or above, $(SSB)_{65}$ binding mode is mostly observed [9]. Single molecule

experiments demonstrated that SSB binding to ssDNA is not static, rather, it diffuses randomly back and forth along ssDNA [10]. A recent molecular dynamics (MD) simulation study revealed that spontaneous formation of ssDNA bulges and their diffusive motion along SSB surface facilitates the dynamic nature of the ssDNA SSB interaction [11]. SSB plays direct role in the DNA replication and recombination [12]. During recombination, SSB helps in heteroduplex formation by binding to the displaced stand and preventing strand annealing [13]. Under physiological conditions in vitro, all of the SSB binding modes exists in dynamic equilibrium on long ssDNA [14].

AlkB-catalyzed oxidative demethylation reaction has been studied in detail using various oligonucleotide substrates [7, 15-22]. *E. coli* SSB molecules are present abundantly enough to bind to all the ssDNA. Role of SSB in some of the DNA repair pathways including base excision repair and recombination repair is known [23-25]. We have recently reported AlkB-mediated repair of alkyl-adducts in SSB-bound ssDNA [26]. By using SSB crystal structure [27] and MD simulation we prove that the specific binding of AlkB with SSB-bound DNA leads to a conformation of AlkB which might promote effective repair of SSB-coated substrate. Our data revealed that SSB-bound DNA could indeed be the substrate for AlkB.

MATERIALS AND METHODS

Molecular docking analysis of AlkB with ssDNA bound SSB. The atomic coordinates of the protein files namely AlkB (3I49), and SSB (1EYG) were retrieved from Protein Data Bank. The protein structures were solvated in a pre-equilibrated cubic TIP3P water box using the CHARMM-GUI [28]. The input files for equilibration and minimization were generated through

Quick MD Simulator in CHARMM-GUI which is a web-based graphical user interface to convert a PDB file to CHARMM readable files. The structure of ssDNA bound SSB and AlkB were equilibrated and energy minimized using GROMACS 4.6.5 using the steepest descent algorithm [29] with CHARMM36 force filed [30]. The minimized structures were then docked using HADDOCK (High Ambiguity Driven protein-protein DOCKing) which is an information-driven flexible docking approach for the docking of biomolecular complexes [31, 32]. The structure of SSB bound ssDNA and AlkB was minimized using GROMACS 4.6. HADDOCK clustered 395 structures in 6 clusters, which represents 98.75 % of the water-refined models generated. Docking analysis was performed to identify the possible conformations of the AlkB protein around SSB ssDNA complex. The docked poses were analyzed for non-covalent interactions namely hydrogen bonding, van der Waals interactions and hydrophobic interactions using Maestro Schrodinger suite (Schrödinger, LLC, New York, NY, 2014).

Molecular Dynamics Simulation. Molecular dynamics simulations was performed for 3 systems namely; AlkB alone (PDB ID: 3I49), ssDNA-SSB complex (PDB ID: 1EYG) and AlkB-SSB-ssDNA docked complex for 50ns with GROMACS version 4.5.4 [33] using CHARMM27 force field parameters. This force field has been widely used for macromolecule simulation [34]. All the systems were first solvated with 40048 TIP3P [35] water molecules in a 11 × 11 × 11 nm3 cubic box. Initially, the energy minimizations of the system were carried out using the steepest descent algorithm [29]. Subsequently, all systems were subjected to a two-step equilibration phase namely; NVT (constant number of particles, Volume and Temperature) for 100 ps to stabilize the temperature of the system and NPT. All simulations were carried out in the isothermal–isobaric ensemble, and protein were kept unconstrained throughout simulations.

The pressure was controlled at 1atm, and the temperature was retained at 310K using a Parrinelo-Rahman barostat and V-rescale thermostat, respectively [36-38]. A 2 fs time step was used to integrate the equation of motion. Electrostatic interaction was calculated using particle mesh Ewald sums with a nonbonded cutoff 10Å [39]. Bonds between hydrogen and heavy atoms were constrained at their equilibrium length using the LINCS algorithm [40]. Initially, the energy minimizations of the system were carried out followed by the equilibration of all the systems for 200ps. Later, a production run of 50ns was performed in all the systems. The 0.15M NaCl was added to mimic the physiological conditions The trajectories were saved at 10 ps interval for further analysis. The analysis of the trajectories was made using GROMACS suite of programs and visual molecular dynamics (VMD) [41].

Post processing MD. The analysis of the trajectories was performed using GROMACS suite of programs and visual molecular dynamics (VMD) [41]. The root mean square deviation (RMSD) was calculated using and root mean square fluctuation (RMSF) analysis using g_rmsd and g_rms respectively. The images were generated using PyMoL software package (W. L. Delano, The PyMOL Molecular Graphics System, 2002). The ligplot showing 2D interactions were generated using the Schrodinger Maestro package.

Calculation of free energy of binding. After MD simulation of AlkB-ssDNA-SSB for 50ns, the complex was preprocessed using Maestro [42]. The Bimolecular Association with Energetics (eMBrAcE) developed by Schrödinger (MacroModel v11.5) was employed to calculate the binding free energy of ssDNA bound SSB with AlkB using OPLS force-field [43]. This program calculates free energy of binding which includes solvation energy, van der Waals energy,

electrostatic energy, valence energy, and constraint energy. The Embrace calculation was performed on energy difference mode to estimate energy changes upon association.

RESULTS AND DISCUSSION

Structural model of the AlkB-SSB-ssDNA

We have recently shown that when AlkB repairs SSB-bound alkylated ssDNA[26]. This could be challenging for AlkB because 65 nucleotide of ssDNA strand is wrapped around *E. coli* SSB akin to "baseball seam" structure [44]. We first wanted to investigate whether AlkB can interact with SSB-bound ssDNA in the same way as free ssDNA. For this, we decided to make a structural model of AlkB-SSB-ssDNA. We used available structure of *E. coli* AlkB (PDB: 3I49) and tetrameric SSB wrapped by two 35-mer oligo-dC (PDB: 1EYG). Because we wanted to incorporate experimentally proven flexibility of the N-terminal nucleic acid recognition loop of AlkB in our model, we used High Ambiguity Driven protein Docking (HADDOCK) [31, 32] to build AlkB-SSB-DNA model. The final structure was obtained by last snapshot of MD simulation with CHARMM27 force field for 50ns in physiologically relevant solvent condition using the initial 3D model of AlkB-SSB-ssDNA ternary complex (Figure 1A). We have performed three MD runs including AlkB alone, ssDNA-SSB complex and AlkB-SSB-ssDNA docked complex for 50 ns. We have simulated the energy minimized structure of free AlkB as a positive control to understand the structural changes associated with AlkB when associated with ssDNA-SSB complex. Similarly, we have simulated ssDNA-SSB structure as positive control to understand the structural changes of ssDNA in AlkB-ssDNA-SSB ternary complex. All MD simulations were carried out using the same protocol so not to introduce any bias. The Ramachandran plot of the MD optimized structure of AlkB-SSB-ssDNA showed that 99.8%

residues in allowed regions (Figure 1B). Furthermore, 93.7% residues were placed in the most favored regions in the MD-optimized structure, higher than the percentage of residues (88.8%) in the initial model, indicating greater stability of the optimized AlkB-SSB-ssDNA ternary complex structure. The total free energy of binding for simulated structure of AlkB-ssDNA-SSB complex was calculated by EMBRACE of MacroModel version 11.5 module of Schrodinger suite 2017. The Bimolecular Association with Energetics (MBAE), which is the energy changes upon association, was found to be -117.25 kJ/mol for ssDNA with AlkB in the presence SSB.

Interaction between SSB-bound DNA and AlkB

The key feature of AlkB structure is the canonical double-stranded beta-helix (DSBH) domain. The DSBH comprises a large β-sheet and a minor β-sheet. The minor β-sheet contains the Fe-coordinating residues (H131, D133, H187), which comprises a predominantly hydrophobic substrate-binding pocket [22]. Previous studies of AlkB structure also revealed that interaction of Arg161 with the phosphate backbone of damaged base is essential for the recognition of substrate [18, 45, 46]. By performing MD simulation experiment we wanted to know whether a nucleotide base from SSB-bound DNA could find its way into the active site of AlkB. First, closer examination of our AlkB-SSB-ssDNA MD-simulated structure revealed that a DNA base (Cyt-109) of SSB-bound DNA was located in the substrate-binding pocket of AlkB. The stereo image (Figure 1C) of 50ns MD-simulated AlkB-SSB-ssDNA structure illustrates the amino acids from AlkB interacting with Cyt109. The key residues namely T51, W69, Y76 and R161 are important for substrate recognition and DNA binding. Holland et al have reported that mutation of each of these amino acids to alanine has reduced the DNA binding as well as the catalytic activity of AlkB [18]. They have shown that R161 forms hydrogen bond the with the phosphate

of the methylated ssDNA and R161A mutation of the AlkB protein shows 5-fold decrease in affinity for damaged DNA, indicating that this residue has a very important role in the binding of the damaged base. Similarly, our model of AlkB in complex with SSB-ssDNA we observe that residue R161 forms hydrogen bond with Cyt109. During the MD simulation we found that this interaction between Arg161 and phosphate group of Cyt-109 of DNA remained stable. It is also reported that Y76 of AlkB forms Hydrogen bond with the substrate and clamps the base into position for catalysis [18]. In agreement with this study we also observe that Y76 is involved in Hydrogen bond with Cyt109. This result suggests that when AlkB encounters SSB-bound ssDNA, AlkB adopts a conformation that could closely fit a DNA base into the enzyme's active site pocket in proximity to the catalytic centre without any hindrance. Second, we examined whether the DNA base of SSB-bound ssDNA was located within a hydrophobic environment inside active site pocket of AlkB. Hunt et al have reported the structure of AlkB in complex with dT-(1-me-dA)-dT trinucleotide substrate wherein they have shown that the alkylated 1-methyladenine substrate was found in a deep, predominantly hydrophobic cavity of AlkB, comprising of various amino acids such as Pro52, Gly53, Met57, Met61, Trp69, Leu118, Leu 128 and Leu130 [22]. Similarly, in our study we observe that Cyt-109 of SSB-ssDNA complex was located within 4.5Å of AlkB hydrophobic cavity comprising of residues namely; Met49, Val50, Pro52, Met57, Leu128, and Leu130. Third, we have analyzed the interaction between Arg161 of AlkB and SSB-bound DNA strand and we observed that Arg161 formed Hydrogen bonding interaction with the 5'-phosphate group of the substrate nucleotide (Cyt109) of SSB-bound DNA strand with a distance of 2.8Å (Figure 1D). During the MD simulation we found that this interaction between Arg161 and phosphate group of Cyt-109 of DNA remained stable

(Supplementary Figure 1). Together, these results support the accuracy of the structural model and indicate that AlkB can bind the SSB-bound DNA in a manner similar to how it binds the DNA base of free ssDNA.

To evaluate overall structural change of DNA binding interface of AlkB in the presence of SSB-DNA, we measured the distance between two reference AlkB residues, namely Gly54 and Asp163. The reason for selecting these two extreme residues was to map the distance from the farthest point of the AlkB active site pocket. Also, it was chosen to understand if the size of AlkB substrate binding pocket would change or remain constant depending on the simulation system. We observed that these residues are 26.8Å apart in the AlkB native structure. When AlkB alone structure was simulated for 50ns, we observed that the distance between these reference point residues had decreased (25.5Å). In contrast, when the SSB-bound DNA was present, the distance between these residues had expanded further (30.1Å) (Figure 1E). These results underscore the inherent structural flexibility AlkB molecule that could allow interaction with SSB-bound ssDNA. The conformational and structural changes along the simulation trajectories that ultimately allow SSB-bound DNA binding is shown in **Movie S1**. From the **Movie S1**, it is obvious that during the MD simulation, the DNA conformation in the SSB bound DNA system adjusts significantly, indicating strains in the DNA conformation stabilized by the crystalline environment.

Flexibility and stability of AlkB-SSB-ssDNA structural model

The MD simulation allowed us to study stability and flexibility of modelled AlkB-SSB-ssDNA structure. The stability of this structure during the MD simulation was measured by its deviation from the initial structure in terms of Root mean square deviations (RMSD). The RMSD of

backbone atoms of AlkB protein with respect to their crystallographic coordinates versus entire simulation trajectory for 50ns time were calculated. We noticed that all the structures, including free AlkB, SSB bound DNA and AlkB-SSB-DNA complex, achieved a stable state within 20ns of the trajectory period. RMSD of AlkB was stabilized around a value of □2.2Å with an increase of 1Å (Figure 2A). We have monitored the compactness of AlkB structure using the RMSD (Figure 2B), which was higher when AlkB (average RMSD = 0.140Å) was interacting with SSB and DNA (average RMSD = 0.206Å). We observed that RMSD of SSB bound ssDNA (average RMSD = 0.667Å) to be significantly higher in the presence of AlkB (average RMSD = 0.850Å) (Figure 2C). This result indicates DNA undergoes significant larger structural changes to achieve interaction with AlkB. At 50ns, RMSD of SSB remained almost unchanged (Figure 2B), suggesting that SSB might not be contributing to ssDNA binding of AlkB.

To investigate if there are any particular dynamic AlkB residues during interaction with SSB-bound DNA, RMSF (root mean square fluctuations) of AlkB was analyzed. RMSF depicts the flexibility of the protein residues. The RMSF plot generated is average over the entire simulation trajectory of 50 ns as a function of time. We observed that when AlkB was simulated for 50ns in the presence of SSB bound DNA, Tyr76 residue of AlkB showed decreased RMSF (1.0Å). However, the RMSF of the same residue of free AlkB simulated for 50ns without DNA was much higher (4.3Å) (Figure 2D). This data indicate reduced flexibility of Tyr76 in the presence of substrate. Interestingly, it had been reported that the mutation of Tyr76 to Ala resulted dramatic reduction repair activity [18]. N-terminal region from 1 to 90aa of AlkB has a flexible Nucleotide Recoginition Lid (NRL) that plays a critical role in substrate recognition and binding. Holland et al have reported that the dynamic flexibility of this domain in AlkB is mainly

attributed by Y76 and T51-Y55 loop [18]. Comparison of RMSF of the MD-stabilized structure of AlkB-SSB-ssDNA complex and free AlkB also revealed that, the loop comprising Thr51-Tyr55 was rather flexible when DNA was absent (Figure 2D). This is in good agreement with previous structural studies, which demonstrated that in the presence of the methylated DNA, the Thr51-Tyr55 loop shifted from the active site so that the Tyr76 could interact with the base and stabilize the substrate at the active site [18].

Molecular docking of AlkB to dynamics snapshots of SSB-DNA

As shown in the Movie S1, the SSB-associated DNA was rather flexible. Running MD simulations on SSB-DNA (PDB: 1EYG) allowed us to obtain different conformational snapshots of SSB-bound DNA. To examine how these conformations from the MD simulations trajectories varied from each other with respect to AlkB binding, we performed molecular docking of AlkB (PDB: 3I49) using HADDOCK. We performed MD simulations on SSB-ssDNA complex and taken snapshots every 10ns from 0ns to 50ns trajectories, totaling six snapshots for analysis. The structure of AlkB was energy minimized using GROMACS4.6.5 before docking. Figure 3A illustrates the overall lowest-energy structures of AlkB-SSB-DNA as build by HADDOCK. When we compared different AlkB-SSB-DNA snapshot structures, it was observed that the positions of AlkB with respect to SSB-ssDNA complex were drastically different. Closer examination revealed that all the key features of AlkB-DNA interactions, including a DNA nucleotide base being present in the hydrophobic active site pocket of AlkB and the interaction between Arg161 with the phosphate backbone of damaged base, are conserved in all these dynamics snapshot models of AlkB-SSB-DNA (Figure 3B and Table 1), suggesting that AlkB can bind to multiple conformation of SSB-bound DNA to perform repair

reaction. These results also suggest that more than one AlkB molecule can be in simultaneously interacting with SSB-bound DNA. Furthermore, analysis of the nature of AlkB-SSB interaction among snapshot models of AlkB-SSB-DNA revealed that there was no specific protein-protein interaction or shape-complementary between AlkB and SSB. Lack of very selective binding may also increase the scanning of a damaged nucleotide. However, the SSB structure used here is without the C-terminal domain and binds DNA in SSB_{65} mode. Recent MD-simulation studies have shown that the equilibrium amount of ssDNA bound to SSB depended on the electrolyte concentration but not on the presence of C-terminal domain of the SSB [11]. At present, it is not clear whether AlkB protein could interact with SSB via the C-terminal unstructured domain of SSB. Although our model suggests the possibility of efficient repair of SSB-coated ssDNA, the role of SSB C-termnal domain in AlkB catalyzed demethylation repair remains to be explored. More work is also needed to understand the importance of SSB-AlkB interaction when SSB binds DNA in SSB_{35} mode.

In conclusion, we report the binding of AlkB with SSB using a GROMACS 4.6.5 CHARMM36 force-field simulated docked model of AlkB-SSB-DNA complex. We have found that Cyt109 from ssDNA-SSB complex forms a stable Hydrogen bond with Arg161 and was present in the hydrophobic cavity of AlkB The close proximity of SSB-bound oligonucleotide with the active site residues of AlkB is explained. This Data will help to understand the binding of flexible SSB-DNA complex with AlkB for potential DNA repair function.

Funding and Acknowledgement

The work was funded by Extra-mural research project (EMR/2016/005135) funded by Science and Engineering Research Board (SERB), Government of India. Authors declare no conflict of interest.

References

[1] Drablos, F., Feyzi, E., Aas, P.A., Vaagbo, C.B., Kavli, B., Bratlie, M.S., et al. Alkylation damage in DNA and RNA--repair mechanisms and medical significance. DNA Repair (Amst). 2004, 3, 1389-407.
[2] Aas, P.A., Otterlei, M., Falnes, P.O., Vagbo, C.B., Skorpen, F., Akbari, M., et al. Human and bacterial oxidative demethylases repair alkylation damage in both RNA and DNA. Nature. 2003, 421, 859-63.
[3] Shen, L., Song, C.X., He, C., Zhang, Y. Mechanism and function of oxidative reversal of DNA and RNA methylation. Annu Rev Biochem. 2014, 83, 585-614.
[4] Yi, C., Jia, G., Hou, G., Dai, Q., Zhang, W., Zheng, G., et al. Iron-catalysed oxidation intermediates captured in a DNA repair dioxygenase. Nature. 2010, 468, 330-3.
[5] Yang, Y., Nair, J., Barbin, A., Bartsch, H. Immunohistochemical detection of 1,N(6)-ethenodeoxyadenosine, a promutagenic DNA adduct, in liver of rats exposed to vinyl chloride or an iron overload. Carcinogenesis. 2000, 21, 777-81.
[6] Sundheim, O., Talstad, V.A., Vagbo, C.B., Slupphaug, G., Krokan, H.E. AlkB demethylases flip out in different ways. DNA repair. 2008, 7, 1916-23.
[7] Falnes, P.O., Bjoras, M., Aas, P.A., Sundheim, O., Seeberg, E. Substrate specificities of bacterial and human AlkB proteins. Nucleic acids research. 2004, 32, 3456-61.
[8] Raghunathan, S., Kozlov, A.G., Lohman, T.M., Waksman, G. Structure of the DNA binding domain of E. coli SSB bound to ssDNA. Nat Struct Biol. 2000, 7, 648-52.
[9] Lohman, T.M., Overman, L.B. Two binding modes in Escherichia coli single strand binding protein-single stranded DNA complexes. Modulation by NaCl concentration. J Biol Chem. 1985, 260, 3594-603.
[10] Roy, R., Kozlov, A.G., Lohman, T.M., Ha, T. SSB protein diffusion on single-stranded DNA stimulates RecA filament formation. Nature. 2009, 461, 1092-7.
[11] Maffeo, C., Aksimentiev, A. Molecular mechanism of DNA association with single-stranded DNA binding protein. Nucleic Acids Res. 2017, 45, 12125-39.
[12] Meyer, R.R., Laine, P.S. The single-stranded DNA-binding protein of Escherichia coli. Microbiol Rev. 1990, 54, 342-80.
[13] Shereda, R.D., Kozlov, A.G., Lohman, T.M., Cox, M.M., Keck, J.L. SSB as an organizer/mobilizer of genome maintenance complexes. Crit Rev Biochem Mol Biol. 2008, 43, 289-318.
[14] Roy, R., Kozlov, A.G., Lohman, T.M., Ha, T. Dynamic structural rearrangements between DNA binding modes of E. coli SSB protein. J Mol Biol. 2007, 369, 1244-57.

[15] Delaney, J.C., Smeester, L., Wong, C., Frick, L.E., Taghizadeh, K., Wishnok, J.S., et al. AlkB reverses etheno DNA lesions caused by lipid oxidation in vitro and in vivo. Nature structural & molecular biology. 2005, 12, 855-60.
[16] Falnes, P.O. Repair of 3-methylthymine and 1-methylguanine lesions by bacterial and human AlkB proteins. Nucleic acids research. 2004, 32, 6260-7.
[17] Falnes, P.O., Johansen, R.F., Seeberg, E. AlkB-mediated oxidative demethylation reverses DNA damage in Escherichia coli. Nature. 2002, 419, 178-82.
[18] Holland, P.J., Hollis, T. Structural and mutational analysis of Escherichia coli AlkB provides insight into substrate specificity and DNA damage searching. PLoS One. 2010, 5, e8680.
[19] Mishina, Y., Lee, C.H., He, C. Interaction of human and bacterial AlkB proteins with DNA as probed through chemical cross-linking studies. Nucleic Acids Res. 2004, 32, 1548-54.
[20] Mishina, Y., Yang, C.G., He, C. Direct repair of the exocyclic DNA adduct 1,N6-ethenoadenine by the DNA repair AlkB proteins. Journal of the American Chemical Society. 2005, 127, 14594-5.
[21] Welford, R.W., Schlemminger, I., McNeill, L.A., Hewitson, K.S., Schofield, C.J. The selectivity and inhibition of AlkB. The Journal of biological chemistry. 2003, 278, 10157-61.
[22] Yu, B., Edstrom, W.C., Benach, J., Hamuro, Y., Weber, P.C., Gibney, B.R., et al. Crystal structures of catalytic complexes of the oxidative DNA/RNA repair enzyme AlkB. Nature. 2006, 439, 879-84.
[23] Han, E.S., Cooper, D.L., Persky, N.S., Sutera, V.A., Jr., Whitaker, R.D., Montello, M.L., et al. RecJ exonuclease: substrates, products and interaction with SSB. Nucleic Acids Res. 2006, 34, 1084-91.
[24] Handa, P., Acharya, N., Varshney, U. Chimeras between single-stranded DNA-binding proteins from Escherichia coli and Mycobacterium tuberculosis reveal that their C-terminal domains interact with uracil DNA glycosylases. J Biol Chem. 2001, 276, 16992-7.
[25] Umezu, K., Kolodner, R.D. Protein interactions in genetic recombination in Escherichia coli. Interactions involving RecO and RecR overcome the inhibition of RecA by single-stranded DNA-binding protein. J Biol Chem. 1994, 269, 30005-13.
[26] Nigam, R., Anindya, R. Escherichia coli single-stranded DNA binding protein SSB promotes AlkB-mediated DNA dealkylation repair. Biochem Biophys Res Commun. 2018, 496, 274-9.
[27] Ollis, D., Brick, P., Abdel-Meguid, S.S., Murthy, K., Chase, J.W., Steitz, T.A. Crystals of Escherichia coli single-strand DNA-binding protein show that the tetramer has D2 symmetry. J Mol Biol. 1983, 170, 797-800.
[28] Jo, S., Kim, T., Iyer, V.G., Im, W. CHARMM-GUI: a web-based graphical user interface for CHARMM. J Comput Chem. 2008, 29, 1859-65.
[29] Petrova, S.S., Solovev, A.D. The Origin of the Method of Steepest Descent. Historia Mathematica. 1997, 24, 361-75.
[30] Hess, B., Kutzner, C., van der Spoel, D., Lindahl, E. GROMACS 4: Algorithms for Highly Efficient, Load-Balanced, and Scalable Molecular Simulation. J Chem Theory Comput. 2008, 4, 435-47.

[31] Dominguez, C., Boelens, R., Bonvin, A.M. HADDOCK: a protein-protein docking approach based on biochemical or biophysical information. J Am Chem Soc. 2003, 125, 1731-7.
[32] van Zundert, G.C., Rodrigues, J.P., Trellet, M., Schmitz, C., Kastritis, P.L., Karaca, E., et al. The HADDOCK2.2 Web Server: User-Friendly Integrative Modeling of Biomolecular Complexes. J Mol Biol. 2016, 428, 720-5.
[33] Pronk, S., Pall, S., Schulz, R., Larsson, P., Bjelkmar, P., Apostolov, R., et al. GROMACS 4.5: a high-throughput and highly parallel open source molecular simulation toolkit. Bioinformatics. 2013, 29, 845-54.
[34] Lopes, P.E., Roux, B., Mackerell, A.D., Jr. Molecular modeling and dynamics studies with explicit inclusion of electronic polarizability. Theory and applications. Theor Chem Acc. 2009, 124, 11-28.
[35] Berendsen, H.J., Van Gunsteren, W.F., Zwinderman, H.R., Geurtsen, R.G. Simulations of proteins in water. Ann N Y Acad Sci. 1986, 482, 269-86.
[36] Parrinello, M., Rahman, A. Polymorphic transitions in single crystals: A new molecular dynamics method. Journal of Applied Physics. 1981, 52, 7182.
[37] Nose, S. A unified formulation of the constant temperature molecular dynamics methods. The Journal of Chemical Physics. 1984, 81, 511-9.
[38] Bussi, G., Donadio, D., Parrinello, M. Canonical sampling through velocity rescaling. Journal of Chemical Physics. 2007, 126, 014101.
[39] Essmann, U., Perera, L., Berkowitz, M. L., Darden, T., Lee, H., Pedersen, L. G. A smooth particle mesh ewald method. Jiurnal of Chemical Physics. 1995, 103, 8577-93.
[40] Hess, B., Bekker, H., Berendsen, H. J. C., Fraaije, J. G. E. M. A linear constraint solver for molecular simulations. Journal of Computational Chemistry. 1997, 18, 1463-72.
[41] Humphrey, W., Dalke, A., Schulten, K. VMD: visual molecular dynamics. Journal of Molecular Graphics. 1996, 14, 27-8.
[42] Sastry, G.M., Adzhigirey, M., Day, T., Annabhimoju, R., Sherman, W. Protein and ligand preparation: parameters, protocols, and influence on virtual screening enrichments. J Comput Aided Mol Des. 2013, 27, 221-34.
[43] Guvench, O., Weiser, J., Shenkin, P., Kolossvary, I., Still, W.C. Application of the frozen atom approximation to the GB/SA continuum model for solvation free energy. J Comput Chem. 2002, 23, 214-21.
[44] Antony, E., Weiland, E.A., Korolev, S., Lohman, T.M. Plasmodium falciparum SSB tetramer wraps single-stranded DNA with similar topology but opposite polarity to E. coli SSB. J Mol Biol. 2012, 420, 269-83.
[45] Koivisto, P., Duncan, T., Lindahl, T., Sedgwick, B. Minimal methylated substrate and extended substrate range of Escherichia coli AlkB protein, a 1-methyladenine-DNA dioxygenase. The Journal of biological chemistry. 2003, 278, 44348-54.
[46] Yu, B., Hunt, J.F. Enzymological and structural studies of the mechanism of promiscuous substrate recognition by the oxidative DNA repair enzyme AlkB. Proceedings of the National Academy of Sciences of the United States of America. 2009, 106, 14315-20.

Figure legends

Figure 1. *In silico* investigations of the *E.coli* AlkB-SSB-DNA complex. (A) Model of the *E.coli* AlkB-SSB-DNA complex. Experimentally determined structures of AlkB (PDB: 3I49) and DNA-bound SSB (PDB:1EYG) were energy minimized and docked using HADDOCK. The model was then simulated for 50ns using CHARMM to obtain the model. AlkB is shown in grey, ssDNA backbone is shown in black and the four subunits of SSB were shown in red, purple, green and cyan (B) Ramachandran plot of the MD-simulated AlkB-SSB-DNA homology model. The most favored regions are red. Additionally allowed, generously allowed, and disallowed regions are indicated as yellow, light yellow, and white, respectively. The Ramachandran statistics are fine with 93.7% in the favored region (red), 5.6% in the additionally allowed region (yellow), 0.6% in the generously allowed region (light yellow). (C) A close-up view of the 50ns MD-simulated AlkB-SSB-DNA showing AlkB active site residues and Cyt109 from SSB-bound DNA. (D) 2D diagram showing interaction of AlkB to SSB-bound DNA. 50ns MD-simulated AlkB-SSB-DNA interaction diagram generated using the of the Ligplot, Schrödinger Maestro software. (E) Analysis of distance (Å) between G54 and D163 obtained by superimposition of native structure of AlkB (cyan), 50ns MD-simulated structure isolated AlkB (red), and 50ns MD-simulated model structure SSB-bound AlkB (grey).

Figure 2. Structural data from the MD simulations. (A) Root mean square deviation (RMSD) analysis of trajectories of Alkb as a function of simulation time. Simulation was carried out with isolated AlkB and AlkB present in a complex with SSB-bound DNA. Low values for the black line of unbound simulation indicate that the AlkB was in the closed state. (B) RMSD analysis of trajectories of Cα of SSB as a function of simulation time. Simulation was carried out with isolated SSB and SSB present in a complex with SSB-bound DNA. (C) RMSD analysis of

trajectories of all atom of ssDNA as a function of simulation time. Simulation was carried out with isolated SSB-bound and SSB present in a complex with AlkB. (F) Root mean square fluctuation (RMSF) of trajectories of isolated AlkB and within the SSB-DNA complex. The arrows indicate the most significant difference between the two simulations: a large increase in flexibility of Gly76 residue and small loop comprising residues Thr51-Tyr55 for the unbound simulation.

Figure 3. Docking of AlkB and SSB-DNA at various MD simulation times. SSB-DNA structure (PDB:1EYG) was energy minimized and simulated using CHARMM. MD simulation trajectories at (a) 0ns, (b) 10ns, (c) 20ns, (d) 30ns, (e) 40ns, and (f) 50ns were docked with AlkB (PDB: 3I49) using HADDOCK. These results depict the binding conformations of AlkB to SSB-DNA, as the later undergoes conformational fluctuations during MD simulation. The structure of AlkB is shown in grey, ssDNA backbone is shown in black and the four subunits of SSB were shown in red, purple, green and cyan, respectively. (B) 2D diagram AlkB-SSB-DNA interaction diagram generated using the of the Ligplot of Schrödinger Maestro software.

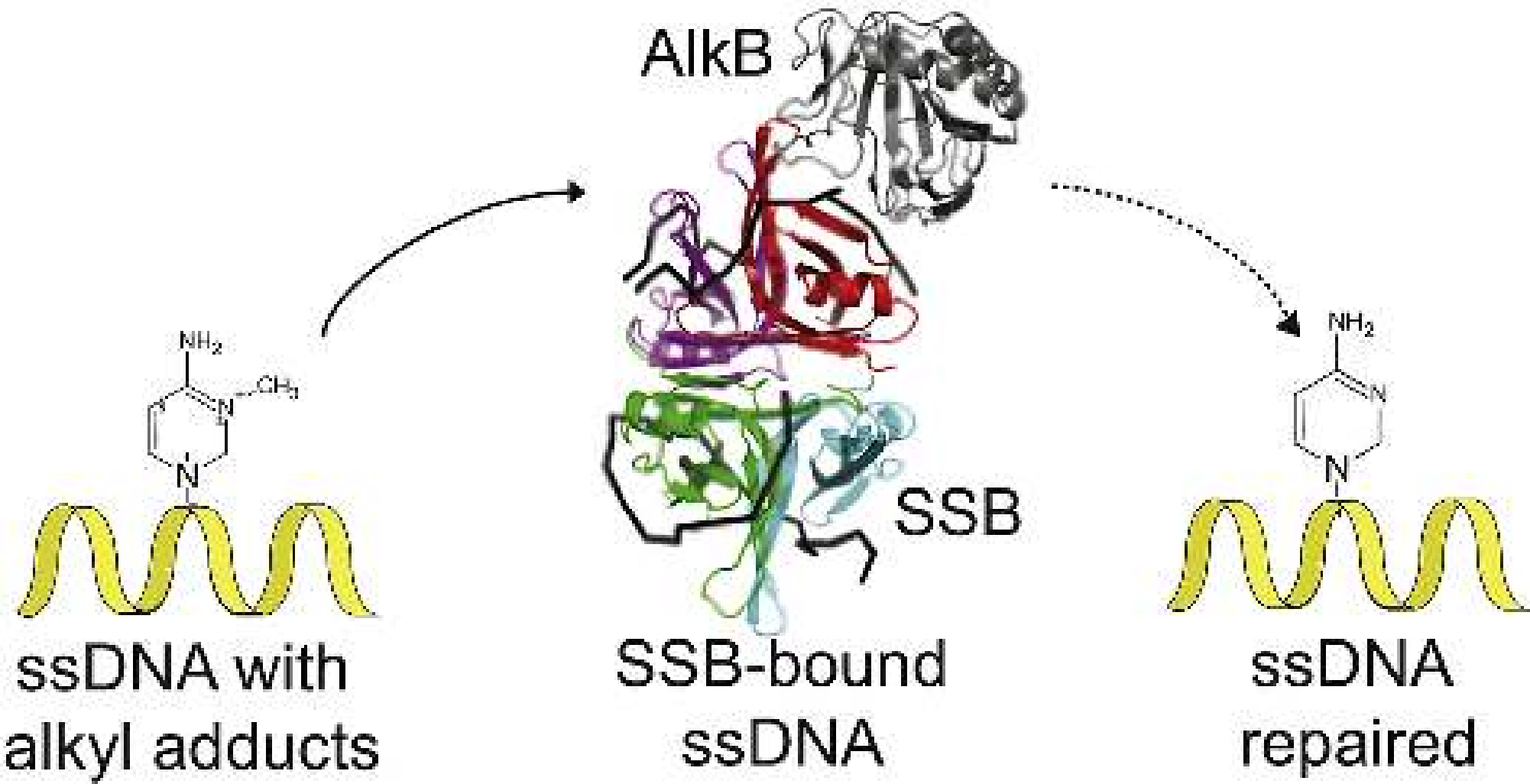
AlkB
SSB
ssDNA with
alkyl adducts
SSB-bound
ssDNA
ssDNA
repaired

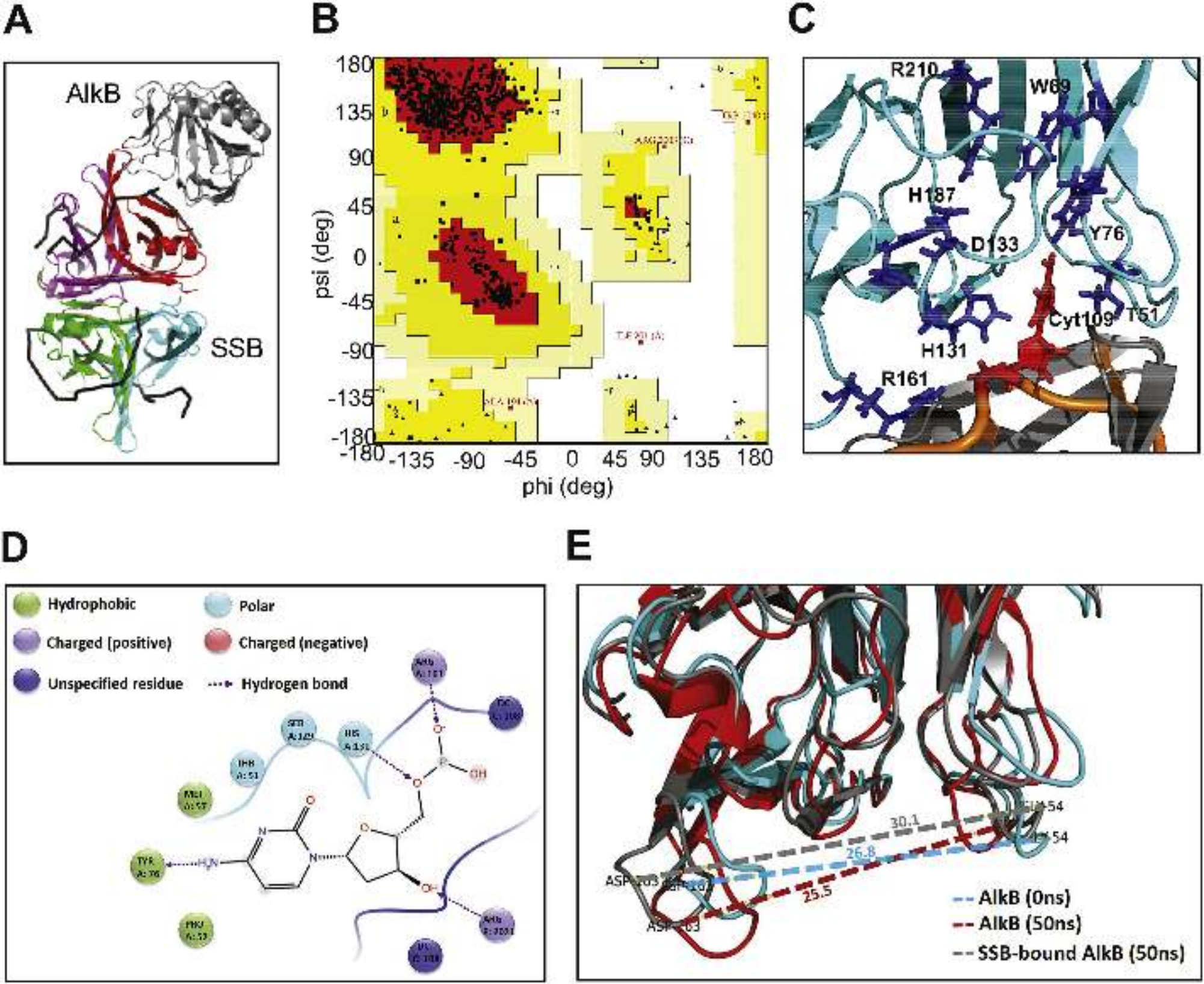
A
AlkB
SSB
B
psi (deg)
phi (deg)
180
135
90
45
0
-45
-90
-135
-180
C
R210
W69
H187
D133
Y76
Cyt109
T51
H131
R161
D
Hydrophobic
Polar
Charged (positive)
Charged (negative)
Unspecified residue
Hydrogen bond
E
30.1
26.8
25.5
AlkB (0ns)
AlkB (50ns)
SSB-bound AlkB (50ns)

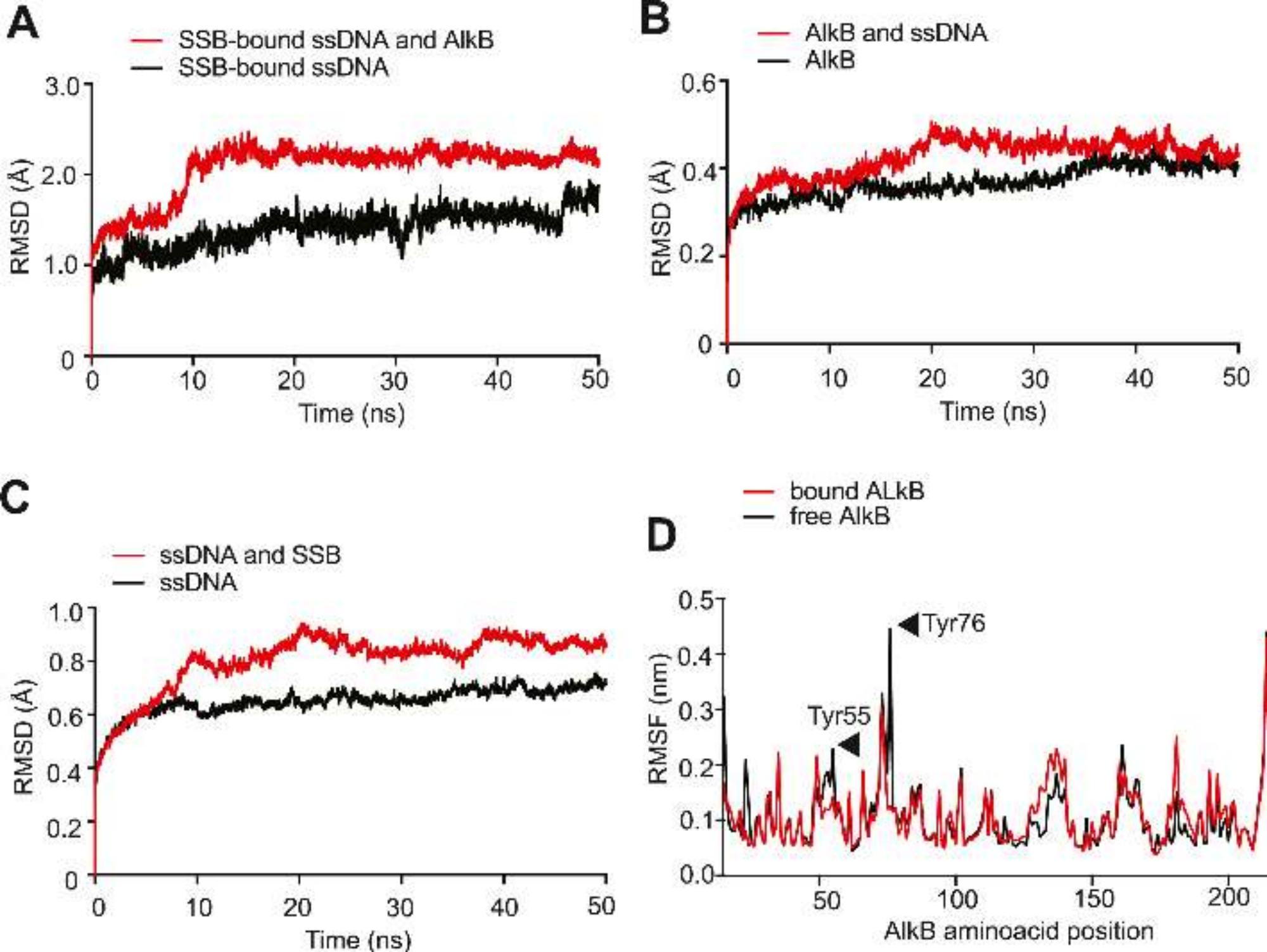
A
SSB-bound ssDNA and AlkB
SSB-bound ssDNA
RMSD (Å)
Time (ns)
B
AlkB and ssDNA
AlkB
RMSD (Å)
Time (ns)
C
ssDNA and SSB
ssDNA
RMSD (Å)
Time (ns)
D
bound ALkB
free AlkB
Tyr76
Tyr55
RMSF (nm)
AlkB aminoacid position

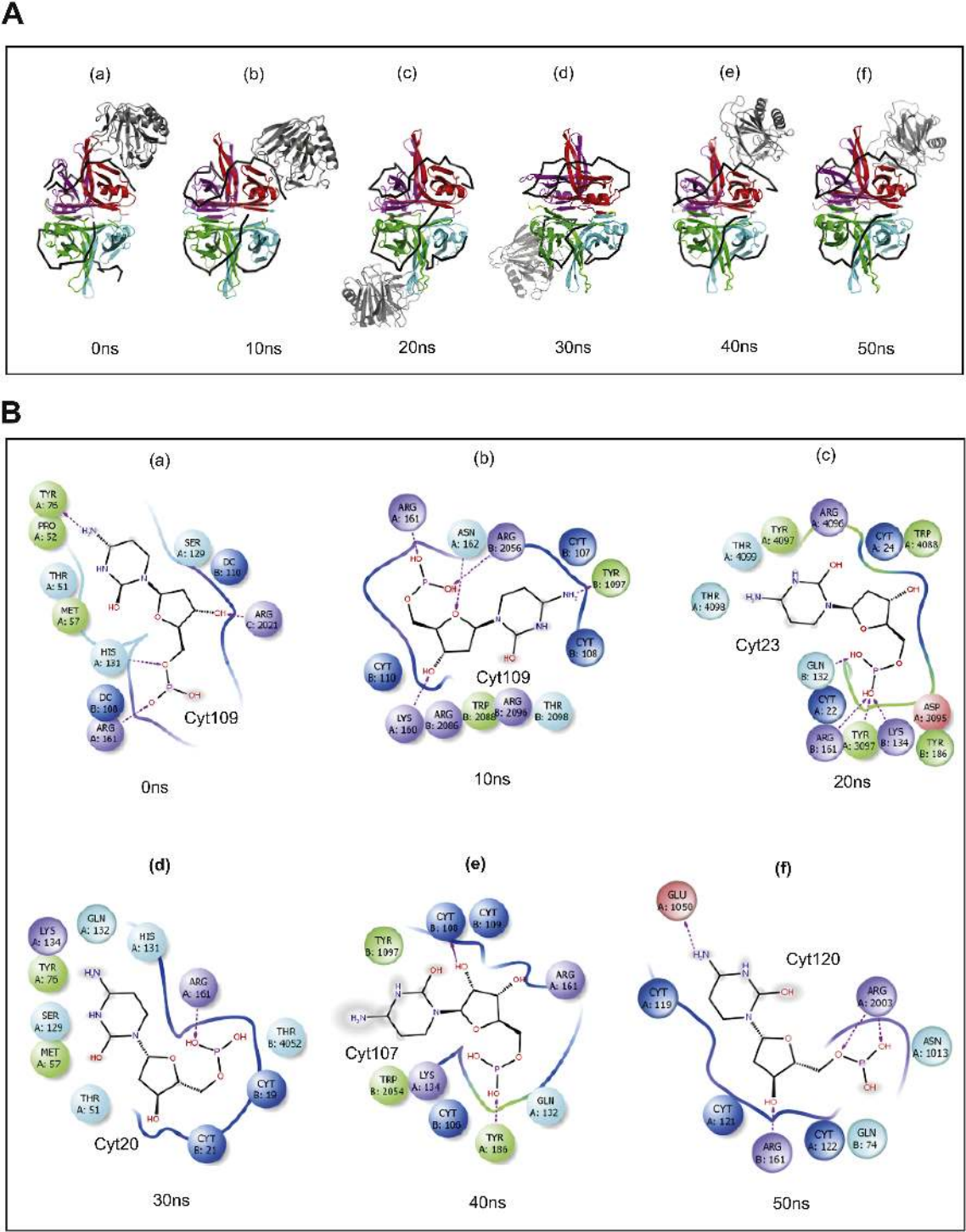
A
(a)
(b)
(c)
(d)
(e)
(f)
0ns
10ns
20ns
30ns
40ns
50ns
B
(a)
(b)
(c)
Cyt109
Cyt109
Cyt23
0ns
10ns
20ns
(d)
(e)
(f)
Cyt20
Cyt107
Cyt120
30ns
40ns
50ns

Research Highlights

- Structural model of *E.coli* DNA repair protein AlkB in SSB-coated ssDNA was generated.
- Molecular Dynamics simulation analysis reveals that AlkB can bind to SSB-bound DNA in multiple ways.
- SSB-bound DNA base could be accessed by AlkB catalytic site.